



Title	Epitaxial growth of Heusler alloy Co ₂ MnSi/MgO heterostructures on Ge(001) substrates
Author(s)	Li, Gui-fang; Taira, Tomoyuki; Matsuda, Ken-ichi; Arita, Masashi; Uemura, Tetsuya; Yamamoto, Masafumi
Citation	Applied Physics Letters, 98(26), 262505 https://doi.org/10.1063/1.3605675
Issue Date	2011-06-27
Doc URL	http://hdl.handle.net/2115/46842
Rights	Copyright 2011 American Institute of Physics. This article may be downloaded for personal use only. Any other use requires prior permission of the author and the American Institute of Physics. The following article appeared in Appl. Phys. Lett. 98, 262505 (2011) and may be found at https://dx.doi.org/10.1063/1.3605675
Type	article
File Information	APL98-26_262505.pdf



[Instructions for use](#)

Epitaxial growth of Heusler alloy $\text{Co}_2\text{MnSi}/\text{MgO}$ heterostructures on $\text{Ge}(001)$ substrates

Gui-fang Li, Tomoyuki Taira, Ken-ichi Matsuda, Masashi Arita, Tetsuya Uemura, and Masafumi Yamamoto^{a)}

Division of Electronics for Informatics, Hokkaido University, Sapporo 060-0814, Japan

(Received 8 April 2011; accepted 10 June 2011; published online 30 June 2011)

We prepared Heusler alloy $\text{Co}_2\text{MnSi}/\text{MgO}$ heterostructures on single-crystal $\text{Ge}(001)$ substrates through magnetron sputtering for Co_2MnSi and electron beam evaporation for MgO as a promising candidate for future generation spin-based functional devices. Structural investigations showed that the $\text{Co}_2\text{MnSi}/\text{MgO}$ heterostructure was grown epitaxially on a $\text{Ge}(001)$ substrate with extremely smooth and abrupt interfaces and showed the $L2_1$ structure for the Co_2MnSi film. Furthermore, a sufficiently high saturation magnetization (μ_s) value of $5.1 \mu_B/\text{f.u.}$ at 10 K, which is close to the theoretically predicted μ_s of $5.0 \mu_B/\text{f.u.}$ for half-metallic Co_2MnSi , was obtained for prepared Co_2MnSi films. © 2011 American Institute of Physics. [doi:10.1063/1.3605675]

There has been growing interest in spintronic devices in which both the charge and spin of the electron are utilized to provide functionalities such as nonvolatility and reconfigurability.¹ In particular, injection of spin-polarized electrons into semiconductor channels and manipulation of the injected spins have been intensively studied recently.^{2–4} A Heusler alloy/ MgO heterostructure is one of the promising candidates as the spin source in spintronic devices, including magnetic tunnel junctions (MTJs) and spin-based semiconductor devices. This is because of (1) the half-metallic nature predicted theoretically for many Heusler alloys^{5–7} and (2) enhanced tunneling spin polarization by coherent tunneling through a single-crystalline $\text{MgO}(001)$ tunnel barrier.^{8,9} Indeed, high tunnel magnetoresistance ratios of 236% at room temperature (RT) and 1135% at 4.2 K of fully epitaxial Co_2MnSi (CMS)/ $\text{MgO}/\text{Co}_2\text{MnSi}$ MTJs have been demonstrated owing to these two characteristics, where the Co_2MnSi thin film was used not only as a lower electrode but also as an upper electrode.^{10,11} In addition, a heterostructure consisting of Heusler alloy upper electrode/ MgO barrier/semiconductor channel is advantageous for spin injection into the semiconductor channel because of the effectiveness of MgO tunnel barrier insertion to solve the conductivity-mismatch problem between a ferromagnetic electrode and a semiconductor channel.¹² As a next-generation semiconductor channel material for metal-oxide-semiconductor devices, germanium (Ge) has attracted much interest because of the high mobility of electrons and holes in Ge.^{13,14} However, previous studies have been restricted to epitaxial growth of Heusler alloy thin films (Fe_2MnSi (Ref. 15) or Co_2MnSi (Ref. 16)) directly on Ge single-crystal substrates and that of ferromagnetic layers on Ge single-crystal substrates via a MgO interlayer only for Fe (Ref. 17) and CoFe .¹⁸ Thus, our purpose in the present study has been to prepare epitaxial Heusler alloy Co_2MnSi films on $\text{Ge}(001)$ substrates, via an ultrathin $\text{MgO}(001)$ interlayer. Note also that the MgO insertion between a Heusler alloy thin film and

a semiconductor provides a barrier against possible interdiffusion between a Heusler alloy thin film and a semiconductor during annealing at about 500 °C.

First, we describe the preparation of the $\text{Co}_2\text{MnSi}/\text{MgO}$ heterostructure. The fabricated layer structure was as follows: (from the upper side) Ru cap (5 nm)/CMS (20 nm)/ MgO interlayer (3 nm), grown on a $\text{Ge}(001)$ single crystal substrate. Before the $\text{Ge}(001)$ substrate was installed in an ultrahigh-vacuum (UHV) chamber, it was oxidized at 500 °C for 1 h and then cleaned with hydrofluoric acid solution. The Ge substrate was then annealed at 650 °C for 1 h in the UHV chamber. All the layers in the heterostructure were successively deposited in the UHV chamber (base pressure of $\sim 6 \times 10^{-8}$ Pa) through the combined use of magnetron sputtering for CMS and electron beam evaporation for MgO . The MgO interlayer was deposited at 125 °C. CMS films were prepared with a Mn-rich composition according to our previous finding that the spin polarization of sputter-deposited CMS films with a Mn-rich composition of $\alpha > 1$ in the $\text{Co}_2\text{Mn}_\alpha\text{Si}$ expression is higher than that of sputter-deposited CMS films with a stoichiometric composition ($\alpha = 1.0$) because of the suppressed Co_{Mn} antisites.¹¹ The CMS layer was deposited by co-sputtering with a nearly stoichiometric CMS target and a Mn target at RT and successively annealed *in situ* at various temperatures, T_a , ranging from 400 °C to 525 °C. The CMS film composition was determined to be $\text{Co}_2\text{Mn}_{1.32}\text{Si}_{0.88}$, i.e., Mn rich with respect to Co, through inductively coupled plasma optical emission analysis with accuracy of 2%–3% for Co and Mn and 5% for Si.

We investigated the structural properties of the fabricated CMS/ $\text{MgO}/\text{Ge}(001)$ heterostructures through cross-sectional high resolution transmission electron microscope (HRTEM) observations, micro-beam electron diffraction, and *in-situ* reflection high-energy electron diffraction (RHEED) observations. Magnetic properties were investigated using a superconducting quantum interference device magnetometer at 10 K and 300 K. The magnetization (M) versus magnetic field (H) curves measured at both 10 K and 300 K for the n -type $\text{Ge}(001)$ substrate showed diamagnetic behavior. Furthermore, we confirmed that the almost linear decrease in M with H in

^{a)}Author to whom corresponding should be addressed. Electronic mail: yamamoto@nano.ist.hokudai.ac.jp.

the H range over about 3 kOe for CMS/MgO/Ge(001) samples could be ascribed to the diamagnetic contribution from the Ge substrates. Thus, the contribution from the Ge substrate was subtracted by extrapolating the M - H curve in the H range over 3 kOe to $H = 0$ to estimate the saturation magnetization for CMS films.

To obtain the saturation magnetization per formula unit (f.u.), μ_s , from that per volume, we had to precisely measure the thickness of CMS films deposited by co-sputtering with a designed thickness of 20 nm. To do this, we performed low-angle x-ray reflectivity measurements. Then the CMS film thickness was determined through the fitting of the experimental low-angle x-ray reflectivity data. The lattice constants in the plane, a , and perpendicular to the plane, c , also had to be determined for the CMS films on MgO/Ge(001) substrates to obtain the μ_s values. However, the x-ray diffraction peaks for CMS and Ge in the prepared CMS/MgO/Ge(001) were not separated because (1) the lattice constant of bulk CMS is equal to that of Ge within about 0.1%, (2) a cube-on-cube crystallographic relationship existed between the CMS layer and the Ge(001) substrate in the prepared CMS/MgO/Ge(001) as described below, and (3) the forbidden Ge diffraction peaks (for example, the Ge(002) and Ge(042) peaks) appeared, probably due to multiple diffraction.¹⁹ On the other hand, if we compare a and c values obtained from the unseparated (002) and (042) diffraction peaks for CMS/MgO/Ge(001) and those obtained for a CMS film on MgO-buffered MgO(001) substrate, the difference is negligible. Thus, we approximated a and c from the values obtained for a CMS film on a MgO-buffered MgO(001) substrate; these films had nominally the same film composition as that of the CMS films used in this study.

Figure 1(a) shows an HRTEM lattice image of a heterostructure consisting of CMS (5 nm)/MgO interlayer (3 nm)/Ge(001) substrate with a co-sputtered $\text{Co}_2\text{Mn}_{1.32}\text{Si}_{0.88}$ film, where the MgO interlayer was deposited at 125 °C and the CMS layer was deposited at RT and successively annealed *in situ* at 500 °C. The electron injection was along the $[1-10]$ direction of the Ge substrate (corresponding to the $[1-10]_{\text{CMS}}$ direction). This image clearly shows that both the MgO interlayer and the CMS layer were grown epitaxially and

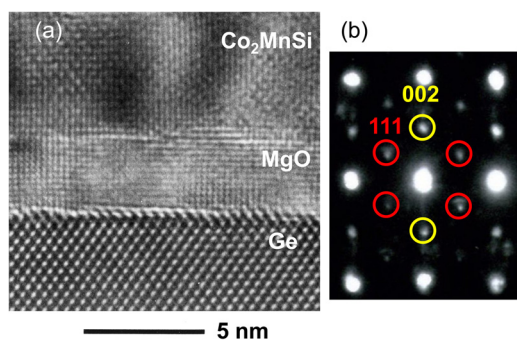


FIG. 1. (Color online) (a) Cross-sectional HRTEM lattice image of a heterostructure consisting of CMS (5 nm)/MgO interlayer (3 nm)/Ge(001) substrate with a co-sputtered $\text{Co}_2\text{Mn}_{1.32}\text{Si}_{0.88}$ film along the $[1-10]$ direction of the Ge substrate (corresponding to the $[1-10]_{\text{CMS}}$ direction), where the CMS film was annealed *in situ* at 500 °C after it was deposited at RT. (b) Electron diffraction pattern for the CMS film (5 nm). The electron beam diameter was 2.5 nm.

were single-crystalline. It also confirmed that extremely smooth and abrupt interfaces were formed. Figure 1(b) shows micro-beam electron diffraction patterns of the CMS film for a beam diameter of 2.5 nm; in these patterns, 111 spots were observed, indicating the L_{21} structure for the CMS thin film prepared by co-sputtering. Note that unidentified spots were superimposed onto the Heusler L_{21} spots in some regions of the CMS thin film, indicating the coexistence of unidentified materials or structures in addition to the Heusler L_{21} structure. This was in agreement with the micro-beam electron diffraction patterns for CMS films grown on MgO-buffered MgO(001) substrates by co-sputtering with a Mn-rich film composition of $\text{Co}_2\text{Mn}_{1.29}\text{Si}_{1.06}$.¹¹

We observed streak patterns dependent on the electron injection direction, parallel to $[100]_{\text{Ge}}$ or $[110]_{\text{Ge}}$, for each successive layer in the CMS/MgO/Ge(001) heterostructure during fabrication through *in-situ* RHEED observations. Furthermore, the spacing of the observed streak patterns of the MgO interlayer agreed well with that of the Ge(001) substrate for both electron injection directions, parallel to $[100]_{\text{Ge}}$ and $[110]_{\text{Ge}}$, indicating that the MgO interlayer was grown epitaxially on a Ge(001) substrate with a crystallographic relationship of $\text{MgO}(001)[110]||\text{Ge}(001)[100]$. The epitaxial relationship of $\text{MgO}(001)[110]||\text{Ge}(001)[100]$ is as expected from the relatively small lattice mismatch (5.2%) between MgO(001) and Ge(001) on a 45° in-plane rotation. This relationship is consistent with previous work on MgO/Ge(001) heterostructures^{17,18} and in contrast to the cube-on-cube epitaxial growth of MgO on GaAs(001)^{20,21} and MgO on Si(001)²² with a 4:3 coincident site lattice.

Similarly, the spacing of the observed streak patterns of the CMS layer agreed well with that of the MgO(001) interlayer for both electron injection directions, parallel to $[100]_{\text{Ge}}$ and $[110]_{\text{Ge}}$, indicating that the CMS film was also grown epitaxially on a MgO(001) interlayer (3 nm)/Ge(001) substrate with a crystallographic relationship of $\text{CMS}(001)[100]||\text{MgO}(001)[110]$. This crystallographic relationship agreed with that obtained for CMS films epitaxially grown on MgO-buffered MgO(001) substrates.²³ Summarizing the obtained relationship from the *in situ* RHEED observations, we concluded that the crystallographic relationship for the prepared CMS/MgO/Ge(001) heterostructure was $\text{CMS}(001)[100]||\text{MgO}(001)[110]||\text{Ge}(001)[100]$.

Next, we describe the magnetic properties of 20-nm-thick CMS films on MgO(001) interlayer (3 nm)/Ge(001) substrates. Magnetic hysteresis curves for a CMS film with $T_a = 500$ °C at 300 K, where H was applied in the plane of the film along the CMS $[1-10]$, $[100]$, and $[110]$ directions, showed that the curves for $[1-10]_{\text{CMS}}$ and $[110]_{\text{CMS}}$ were equivalent. However, the coercive force $H_c = 5$ Oe for $[100]_{\text{CMS}}$ was lower than the $H_c = 20$ Oe for $[1-10]_{\text{CMS}}$ and $[110]_{\text{CMS}}$. These characteristics of the hysteresis curves show the in-plane cubic magnetic anisotropy with easy axes of $\langle 110 \rangle_{\text{CMS}}$ and hard axes of $\langle 100 \rangle_{\text{CMS}}$ for the epitaxial MgO(001) interlayer induced by the cubic crystal symmetry of the single crystalline CMS. Figure 2(a) shows magnetic hysteresis curves for CMS films with various T_a values in the range from 400 to 525 °C up to ± 10 kOe at 10 K, where H was applied in the plane of the film along the $[1-10]_{\text{CMS}}$ easy

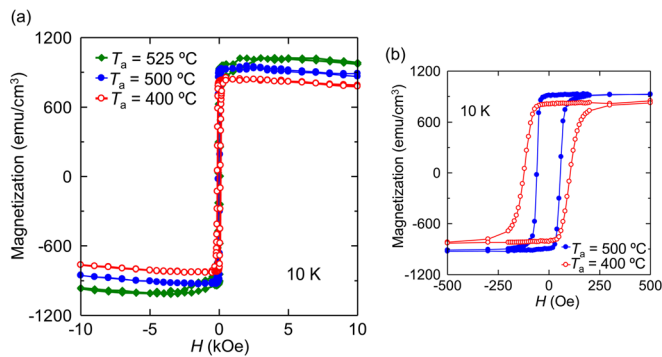


FIG. 2. (Color online) Typical magnetic hysteresis curves for CMS films (20 nm) on MgO interlayer (3 nm)/Ge(001) substrates at 10 K, where H was applied in the plane of the film along the $[1-10]_{\text{CMS}}$ easy axis. (a) Magnetic hysteresis curves for CMS films with various T_a values in the range from 400 to 525 °C up to ± 10 kOe. (b) Magnetic hysteresis curves for CMS films with $T_a = 400$ or 500 °C at 10 K up to smaller magnetic fields of ± 500 Oe.

axis. Magnetic hysteresis curves for CMS films with $T_a = 400$ or 500 °C up to smaller magnetic fields of ± 500 Oe at 10 K are also shown in Fig. 2(b). With increasing T_a from 400 to 525 °C, the saturation magnetization increased and H_c decreased. Along with the decrease in H_c with increasing T_a , the hysteresis curve became more square-like, as shown in Fig. 2(b).

Figure 3 shows μ_s and H_c for CMS films at 10 K and 300 K as a function of T_a . The μ_s values at 10 K increased with increasing T_a from $\mu_s = 4.2 \mu_B/\text{f.u.}$ for $T_a = 400$ °C up to $\mu_s = 5.1 \mu_B/\text{f.u.}$ for $T_a = 525$ °C (the corresponding values at 300 K increased from $\mu_s = 3.7 \mu_B/\text{f.u.}$ for $T_a = 400$ °C to $\mu_s = 4.5 \mu_B/\text{f.u.}$ for $T_a = 525$ °C). The $\mu_s = 5.1 \mu_B/\text{f.u.}$ at 10 K obtained for 525 °C-annealed CMS films was close to the theoretically predicted μ_s of 5.0 $\mu_B/\text{f.u.}$ for half-metallic CMS, and in good agreement with the 5.1 $\mu_B/\text{f.u.}$ for CMS films grown on MgO-buffered MgO(001) substrates with nominally the same film composition. These comparisons indicate that the CMS films prepared on Ge(001) substrates via an ultrathin MgO interlayer possessed sufficiently high μ_s values. The H_c values at 300 K decreased with increasing T_a from $H_c = 42$ Oe for $T_a = 400$ °C to $H_c = 17$ Oe for $T_a = 525$ °C (the corresponding values at 10 K decreased from $H_c = 110$ Oe for $T_a = 400$ °C to 50 Oe for $T_a = 525$ °C). The decrease in H_c with increasing T_a was probably induced by a decrease in the pinning center density for the magnetic domain motion²⁴ with increasing T_a up to 525 °C.

In summary, we prepared epitaxially grown Heusler alloy Co_2MnSi (CMS) films on Ge(001) substrates via a MgO interlayer. A cross-sectional HRTEM lattice image of the CMS (5 nm)/MgO interlayer (3 nm)/Ge(001) heterostructure showed that both MgO and CMS layers were grown epitaxially and were single-crystalline. It also confirmed that extremely smooth and abrupt interfaces were formed. 111 diffraction spots observed for CMS by micro-beam electron diffraction indicated the $L2_1$ structure for CMS films. Furthermore, sufficiently high saturation magnetization (μ_s) values at 10 K close to the theoretically predicted μ_s for half-metallic CMS were obtained for prepared CMS films. These

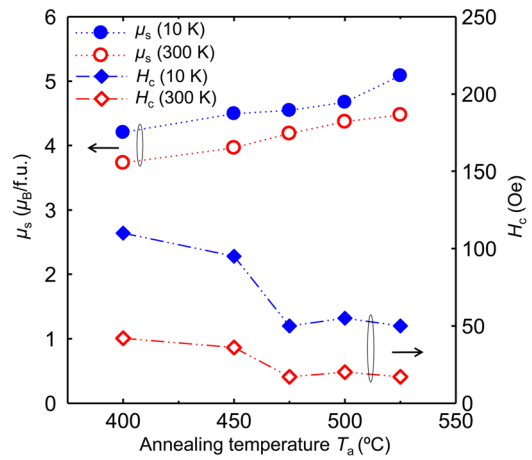


FIG. 3. (Color online) Saturation magnetization per formula unit (μ_s) and coercive force (H_c) for CMS films (20 nm) on MgO(001) interlayer (3 nm)/Ge(001) substrates as a function of T_a at 10 K and 300 K, where H was applied in the plane along the $[1-10]_{\text{CMS}}$ easy axis. The film composition was intentionally Mn-rich $\text{Co}_2\text{Mn}_{1.32}\text{Si}_{0.88}$.

results confirm that fully epitaxial CMS/MgO/Ge(001) heterostructures offer great potential as a key device structure for efficient spin injection into a semiconductor channel of Ge featuring high mobility.

The authors thank H. Watanabe and H. Takakura for their valuable discussions. We also thank Y. Honda, H.-x. Liu, and S. Hirata for experimental help. This work was partly supported by Grants-in-Aid for Scientific Research (Grant Nos. 20246054, 21360140 and 22560001), and a Grant-in-Aid for Scientific Research on Priority Area “Creation and control of spin current” (Grant No. 19048001) from MEXT, Japan, and by the Strategic International Cooperative Program of the Japan Science and Technology Agency (JST).

¹S. A. Wolf *et al.*, *Science* **294**, 1488 (2001).

²X. Lou *et al.*, *Nat. Phys.* **3**, 197 (2007).

³O. M. J. van't Erve *et al.*, *Appl. Phys. Lett.* **91**, 212109 (2007).

⁴S. P. Dash *et al.*, *Nature* **462**, 491 (2009).

⁵S. Ishida *et al.*, *J. Phys. Soc. Jpn.* **64**, 2152 (1995).

⁶S. Picozzi, A. Continenza, and A. J. Freeman, *Phys. Rev. B* **66**, 094421 (2002).

⁷I. Galanakis, P. H. Dederichs, and N. Papanikolaou, *Phys. Rev. B* **66**, 174429 (2002).

⁸W. H. Butler *et al.*, *Phys. Rev. B* **63**, 054416 (2001).

⁹J. Mathon and A. Umerski, *Phys. Rev. B* **63**, 220403(R) (2001).

¹⁰T. Ishikawa *et al.*, *Appl. Phys. Lett.* **95**, 232512 (2009).

¹¹M. Yamamoto *et al.*, *J. Phys.: Condens. Matter* **22**, 164212 (2010).

¹²E. I. Rashba, *Phys. Rev. B* **62**, R16 267 (2000).

¹³M. L. Lee *et al.*, *Appl. Phys. Lett.* **79**, 3344 (2001).

¹⁴C. O. Chui *et al.*, *IEEE Electron Device Lett.* **23**, 473 (2002).

¹⁵K. Ueda *et al.*, *Appl. Phys. Lett.* **93**, 112108 (2008).

¹⁶M. A. I. Nahid *et al.*, *Appl. Phys. Lett.* **96**, 142501 (2010).

¹⁷W. Han *et al.*, *J. Cryst. Growth* **312**, 44 (2009).

¹⁸K.-R. Jeon, C.-Y. Park, and S.-C. Shin, *Cryst. Growth Des.* **10**, 1346 (2010).

¹⁹H. Cole, F. W. Chambers, and H. M. Dunn, *Acta Cryst.* **15**, 138 (1962).

²⁰L. D. Chang *et al.*, *Appl. Phys. Lett.* **60**, 1753 (1992).

²¹S. Kawagishi *et al.*, *J. Appl. Phys.* **103**, 07A703 (2008).

²²G. X. Miao *et al.*, *Appl. Phys. Lett.* **93**, 142511 (2008).

²³H. Kijima *et al.*, *IEEE Trans. Magn.* **42**, 2688 (2006).

²⁴E. C. Stoner and E. P. Wohlfarth, *Phil. Trans. R. Soc. London, Ser. A* **240**, 599 (1948).